Supplement of Clim. Past, 15, 307–334, 2019
https://doi.org/10.5194/cp-15-307-2019-supplement

Climate of the Past
Open Access
EGU

Supplement of

Inconsistencies between observed, reconstructed, and simulated precipitation indices for England since the year 1650 CE

Oliver Bothe et al.

Correspondence to: Oliver Bothe (ol.bothe@gmail.com)

24 January 2019

Contents

1 Introduction

This document presents supplementary Figures for Bothe et al. (2018, "Inconsistencies between observed, reconstructed, and simulated precipitation indices for England since the year 1650 CE", compare, https://www.clim-past-discuss.net/cp-2018-27/). It includes additional time-series plots of the used precipitation and temperature data and different visualisations of the relation between different observation based data sets. It also provides additional information on the parameters and moments of the fitted distributions. Additionally, it shows initial assessments of the reconstruction data of Rinne et al. (2013) and a scaling approach for the $\delta^{18}O$ data of Young et al. (2015). Finally, it shows the extension of the analyses in the main paper to the PMIP3-data set (Schmidt et al., 2011).

2 Observation and paleo-observation based data

Figure 1 presents the observational precipitation series and the Central England Temperature since approximately the year 1650 CE. The different sub-divisions of the England-Wales precipitation show notable similarities (Figure 1g to j). The Figure again highlights the differences in mid- to low-frequency variability in the reconstructions compared to the observational data.

2.1 Pairwise comparisons

Figures 2 and 3 complement the correlation matrix presented in the main manuscript. The pairwise complete correlation matrix in the left panel of Figure 2 differs only slightly from the matrix in the main manuscript over the period 1873 to 1994 CE when all records have data. The correlations between non-overlapping 11-year averages over the period 1767 to 1986 CE in the right panel of Figure 2 mainly illustrate the weak relation between the reconstructions and the other data sets. The observational data sets have relatively strong relations on this time-scale and over this period except for the relationship between the Pode Hole precipitation and the Central England Temperature. The scatterplots in Figure 3 visualize the strong relation between the observational precipitation data sets and the weak relation between the reconstructions and the other data sets.

2.2 Distributional properties of observational data and the regional simulation

Figures 4 to 7 present additional plots for the distributional parameters and properties. The Figures supplement the appendices of the main manuscript. Figures 4 and 5 give the shape and scale parameters for the reconstructions over their full period. Shape parameters become notably larger before approximately the year 1600 CE for Southern-Central England and before approximately the year 1500 CE for East Anglia. The longer perspective highlights that excursions to small scale parameters around the year 1800 CE are rare over the full reconstruction period.

Figure 6 shows the skewness for reconstructions, observations, and the regional simulation, which we don't show in the appendix of the main manuscript. Their evolutions mainly reflect those of the respective shape parameters.

Figure 7 adds the plots for the excess kurtosis of the reconstructions over their full period. These series show that the reconstructions' distributions strongly change between early and late periods.

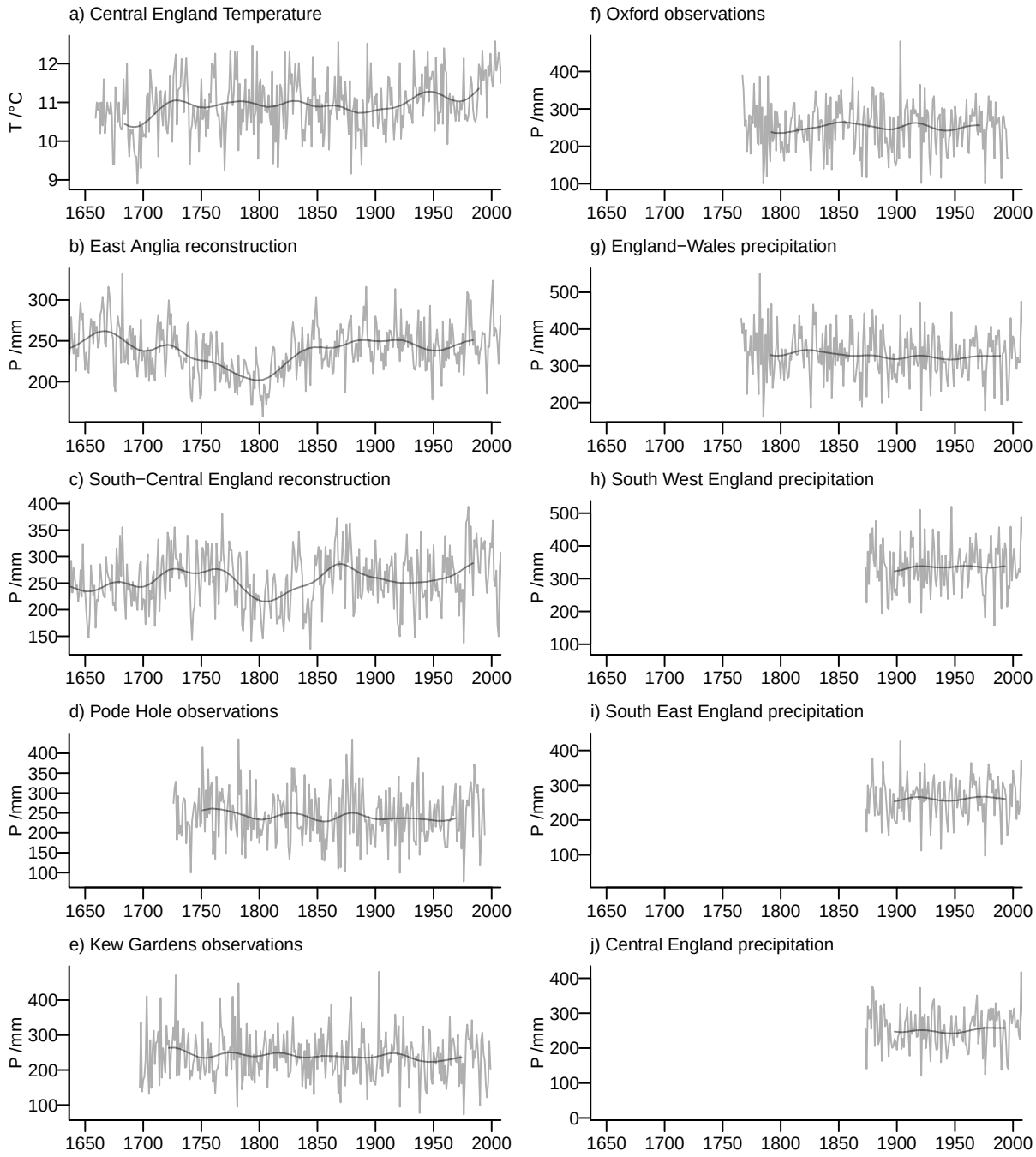

Figure 1: Time-series of interannual and 51-point Hamming-filtered observation based data sets for the extended spring season from March to July (MAMJJ): a) Central England Temperature, b) East Anglia precipitation reconstruction, c) South Central England precipitation reconstruction, d) Pode Hole precipitation observations, e) Oxford precipitation observations, f) Kew Gardens precipitation observations, g) England-Wales precipitation, h) South West England precipitation, i) South East England precipitation, j) Central England precipitation.

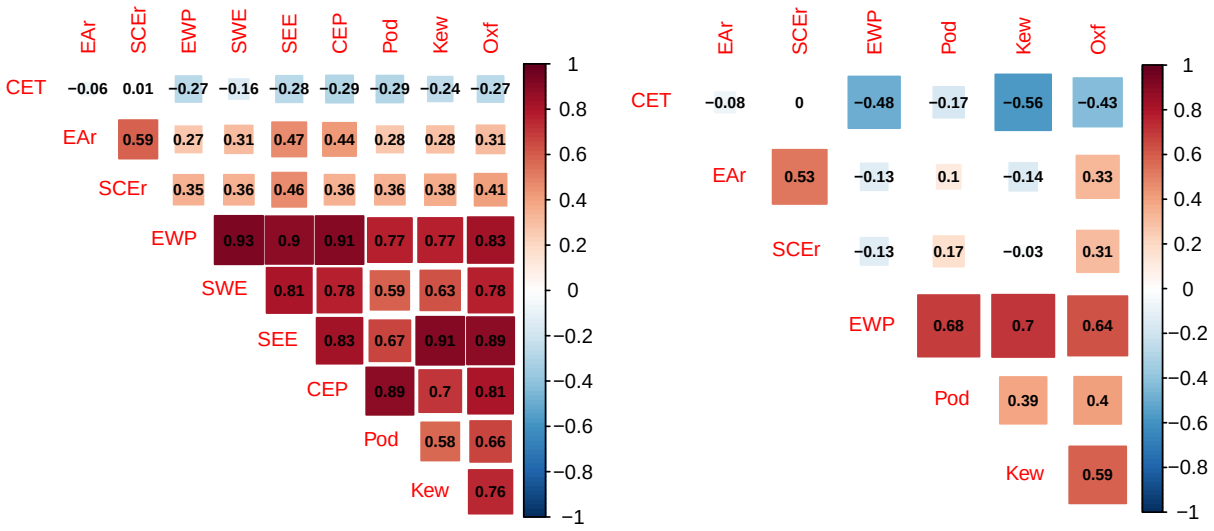

Figure 2: Correlation matrices between the different observation and paleo-observation based data sets for the extended spring season from March to July (MAMJJ). The left panel is for interannual data and pairwise complete data, i.e., correlation coefficients are not directly comparable since they are computed over different periods. The right panel is for non-overlapping 11-year averages for a subset of data between 1767 and 1986 CE. The abbreviations are for Central England Temperature (CET), East Anglia precipitation reconstruction (EAr), Southern-Central England precipitation reconstruction (SCEr), England-Wales precipitation (EWP), South-West England precipitation (SWE), South-East England precipitation (SEE), Central England precipiation (CEP), Pode Hole precipitation (Pod), Kew Gardens precipitation (Kew), and Oxford precipitation (Oxf).

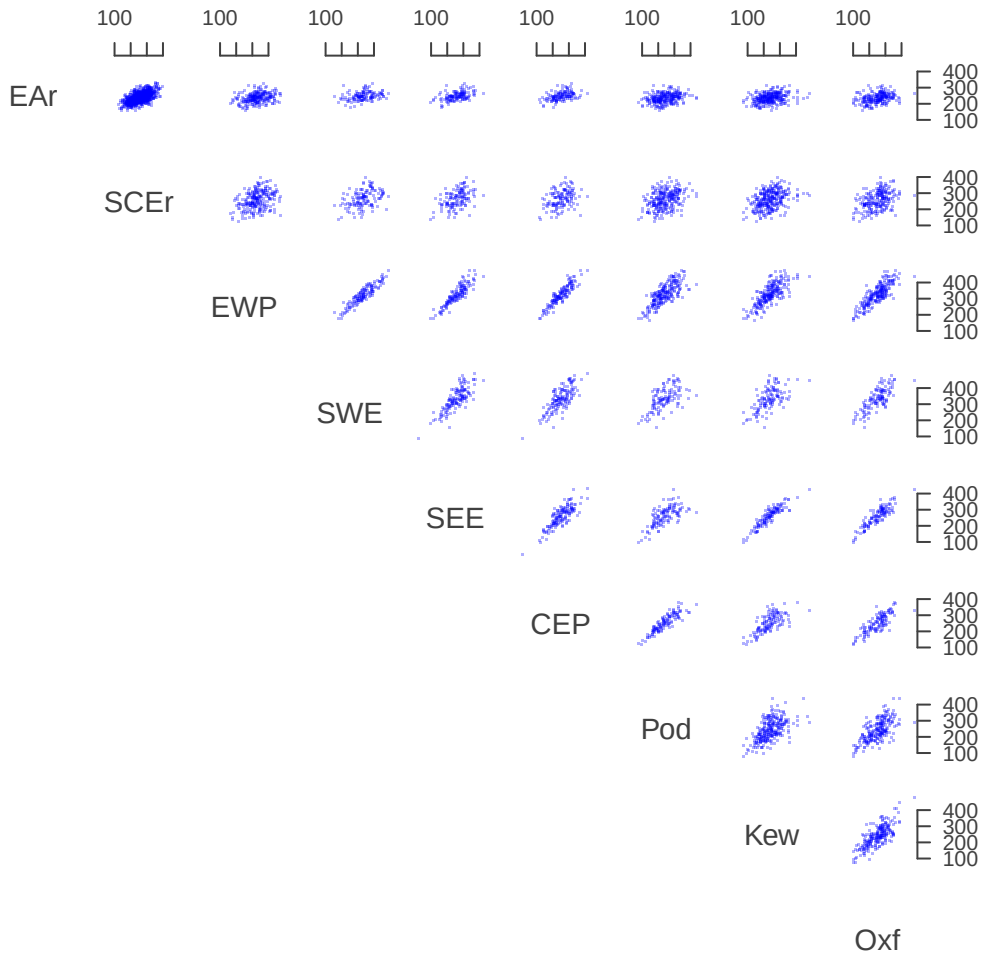

Figure 3: Scatterplots between the various observational precipitation data sets. Plots are for pairwise complete data, i.e., each plot shows different numbers of data-points. Axes are precipitation amounts. The abbreviations are for East Anglia precipitation reconstruction (EAr), Southern-Central England precipitation reconstruction (SCEr), England-Wales precipitation (EWP), South-West England precipitation (SWE), South-East England precipitation (SEE), Central England precipiation (CEP), Pode Hole precipitation (Pod), Kew Gardens precipitation (Kew), and Oxford precipitation (Oxf).

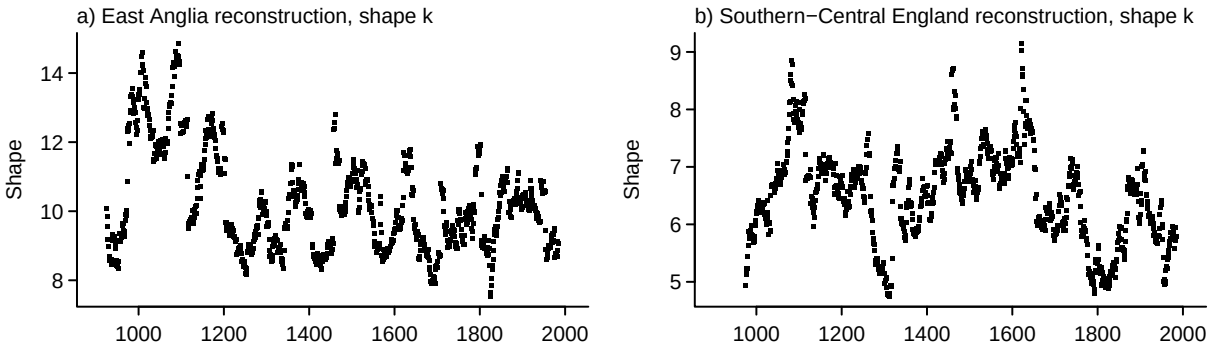

Figure 4: Evolution of shape parameter k for the full reconstruction periods: a) East Anglia, b) Southern-Central England.

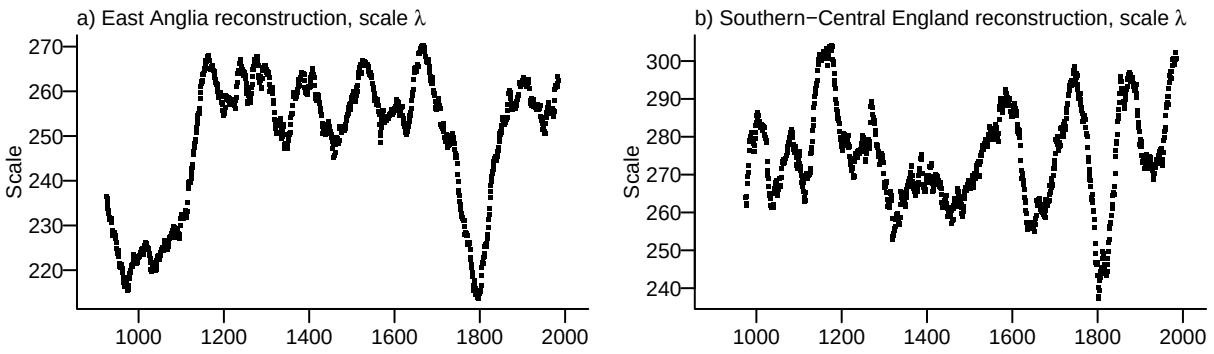

Figure 5: Evolution of scale parameter λ for the full reconstruction periods: a) East Anglia, b) Southern-Central England.

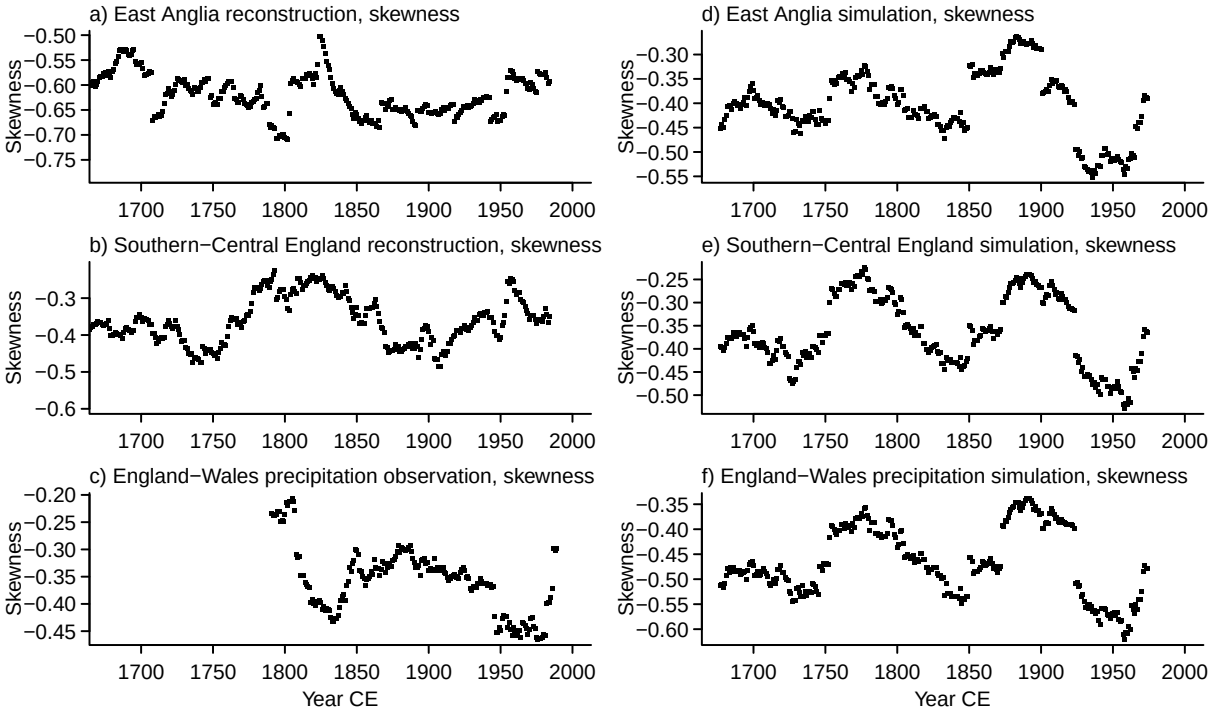

Figure 6: Evolution of the skewness: a) East Anglia reconstruction, b) Southern-Central England reconstruction, c) England-Wales precipitation observational data, d) East Anglia regional simulation, e) Southern-Central England regional simulation, f) England-Wales precipitation regional simulation.

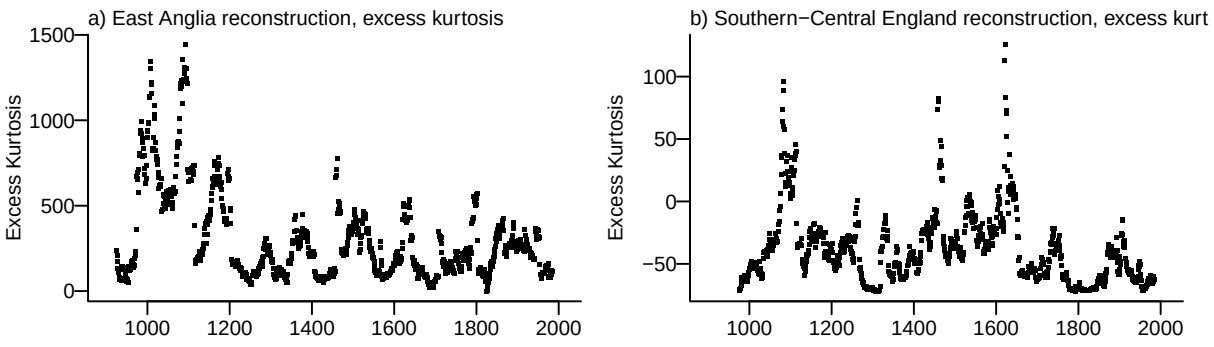

Figure 7: Evolution of the excess kurtosis for the full reconstruction periods: a) East Anglia, b) Southern-Central England.

3 Scaling using Young et al. (2015) $\delta^{18}O$-data

This section shortly discusses a scaling of $\delta^{18}O$ data presented and first used by Young et al. (2015). The supplement of Young et al. (2015) includes their $\delta^{18}O$ data and their manuscript provides enough detail to repeat their suggested reconstruction procedure (compare http://doi.org//10.1007/s00382-015-2559-4 and http://doi.org//10.1007/s00382-015-2559-4#SupplementaryMaterial).

3.1 Original work

Young et al. (2015) collect $\delta^{18}O$-records from Scotland, Wales, and England and reconstruct summer (June-August) precipitation. They use the England-Wales precipitation (Alexander and Jones, 2000) as climate calibration data and for their scaling.

3.2 Input data

We only use the six $\delta^{18}O$-records from Wales and England whereas Young et al. (2015) use eight records. This results in differences in our reconstructed data.

3.3 Scaling of $\delta^{18}O$ data

We apply the scaling procedure described by Young et al. (2015). We rescale the resulting isotope-composite to the mean and variance of the England-Wales precipitation data over the period 1850 to 2006 CE. We show this for the summer (June to August) season but we did another scaling for the extended spring season from March to July. The relation between the chronology and the extended spring precipitation is only weak.

Verification statistics are negative and, thus, the scaling is not skillful in the early period. Our England and Wales composite thereby differs from the England, Wales, and Scotland composite of Young et al. (2015), which retains positive verification also for the early period.

3.4 Results

Figures 8 and 9 present the interannual and smoothed precipitation data for the extended spring season and the summer season respectively. The observed extended spring precipitation in Figure 8d does not show clear similarities to the scaled data in Figure 8c. For summer, the scaled and observed series show some similarities in their mid-frequency variability but there are not any commonalities on longer time-scales. On the other hand, one may see slight similarities between the simulated data and the scaled data for the extended spring, but most prominent are the apparent opposite evolutions recently and in the early part of the records. For summer, there are not any similarities between scaled data and the simulation output (Figure 9).

3.4.1 Percentile series

Figures 10 and 11 show some analyses of the percentiles for the summer season. Since the scaled data sets for both seasons only differ in their mean and their amplitude, we concentrate on summer here.

The wet percentile for the scaled data shows strong deviations from the observations in the beginning of the record and in the early 20th century. Similarly, the dry percentile record deviates strongly before approximately the year 1850 CE but shows slightly more agreement with the observations for the rest of the period.

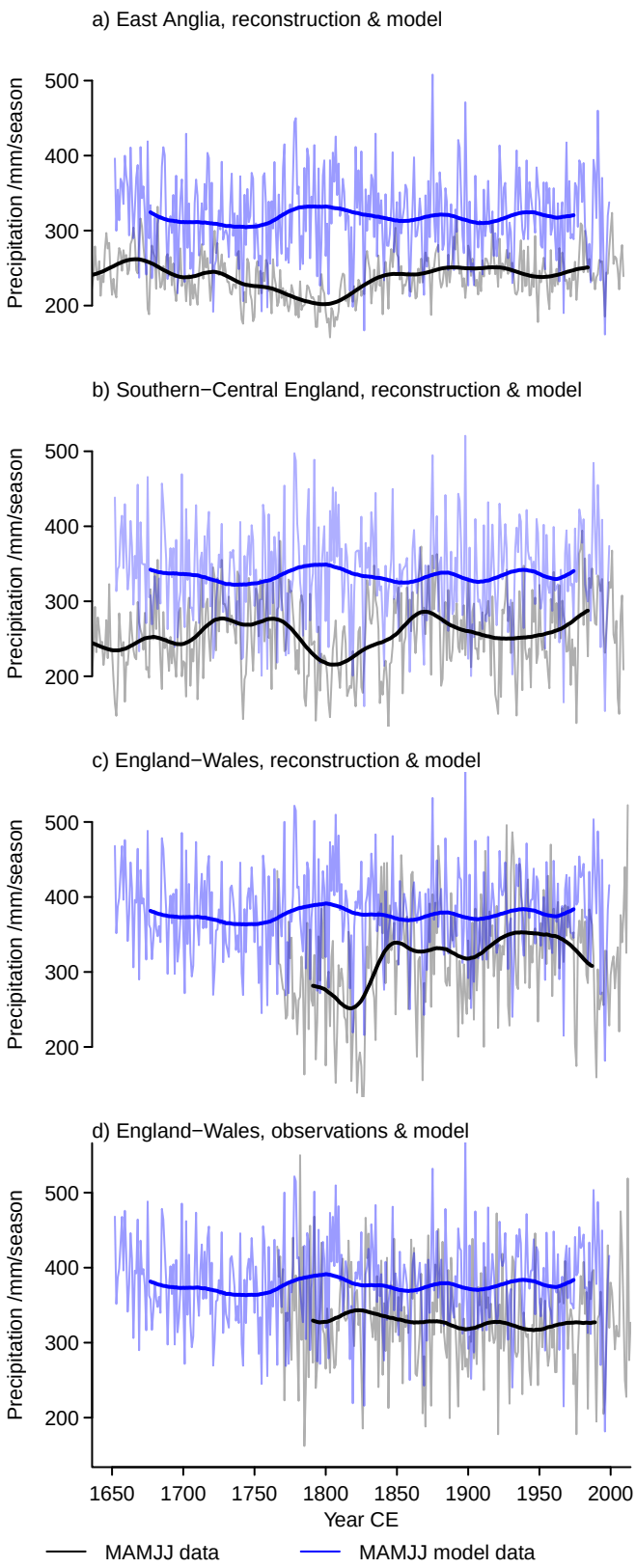

Figure 8: Extended spring (MAMJJ) precipitation in observation based data and simulated data, a) East Anglia precipitation in reconstruction (black) and regional model (blue), b) Southern-Central England precipitation in reconstructions (black) and regional simulation (blue), c) England-Wales scaling reconstruction (black) and regional simulation (blue) and d) England-Wales precipitation in observational data (black) and regional simulation (blue). We show interannual data (transparently colored) and 51-point Hamming-filtered data (solid colored).

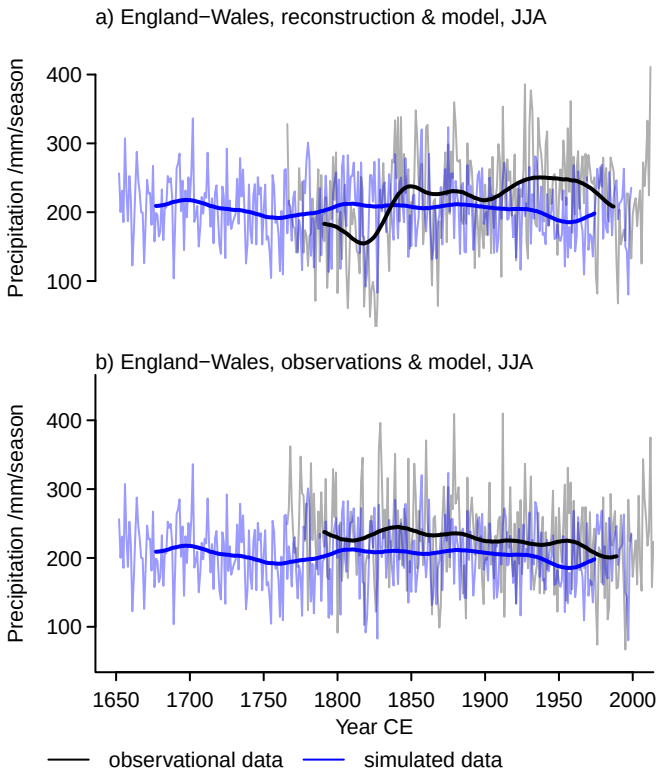

Figure 9: Summer (JJA) precipitation in observation based data and simulated data, a) England-Wales scaling reconstruction (black) and regional simulation (blue) b) England-Wales precipitation in observational data (black) and regional simulation (blue). We show interannual data (transparently colored) and 51-point Hamming-filtered data (solid colored).

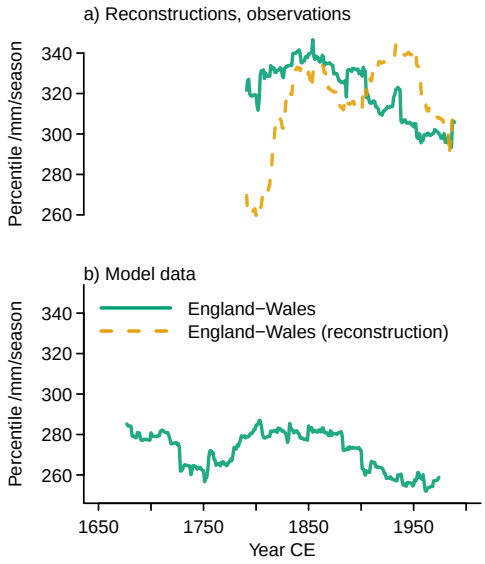

Figure 10: Visualisation of the JJA England-Wales precipitation amount identified as severely wet (93.3th percentile) over 51-year windows for a) reconstructions and observations, and b) regional simulation. Simulation and observations are green solid lines, England-Wales reconstruction is yellow dashed line.

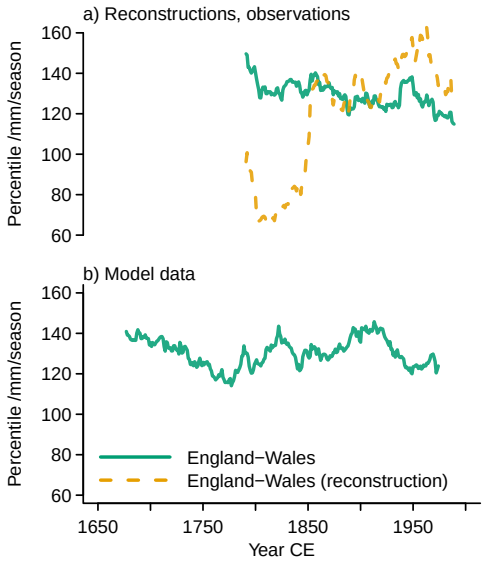

Figure 11: Visualisation of the JJA England-Wales precipitation amount identified as severely dry (6.7th percentile) over 51-year windows for a) reconstructions and observations, and b) regional simulation. Simulation and observations are green solid lines, England-Wales reconstruction is yellow dashed line.

There are not any obvious commonalities between the scaled data and the simulation output and disagreement dominates for summer precipitation. On the other hand, simulated and observed summer precipitation records show similar decreasing trends in their wet percentiles.

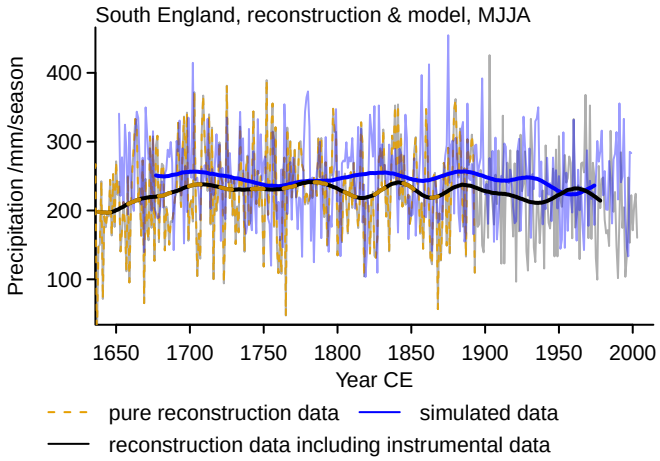

Figure 12: Extended summer (MJJA) precipitation in observation based data and simulated data, South England reconstruction (yellow dashed), South England reconstruction and concatenated observations (black), and regional simulation (blue). We show interannual data (transparently colored) and 51-point Hamming-filtered data (solid colored).

4 Rinne et al. (2013) $\delta^{18}O$-based reconstruction

In the following, we shortly discuss the reconstruction by Rinne et al. (2013). The first author of Rinne et al. (2013) provided their reconstruction data for comparison. Their reconstruction is for an extended summer season from May to August (MJJA). They construct a $\delta^{18}O$ chronology from up to four trees. See their paper for details. They compute a reconstruction by scaling against the station observation data for Radcliffe (cf. Oxford), England. Their record concatenates the Radcliffe instrumental data for 1894 to 2003 CE to the reconstructed values from 1613 until 1893 CE. Thus, the overlap with the England-Wales precipitation data is short. For the simulation data, we use the domain 1.5W to 0E and 51.5N to 52.5N.

4.1 Results

The following concentrates on the reconstructed data and mostly disregards the concatenated observations in the Rinne et al. (2013) record. For moving window measures, plots show data up to the year 1893 CE, i.e. when about half of the window consists of reconstructed values and half the window is observed data.

Figure 12 shows the interannual and 51-point Hamming-filtered records for the simulation and the South England reconstruction. Absolute amounts for extended summer are quite comparable between simulation and reconstruction, although the reconstruction is more or less a point record and the simulation includes a number of grid points. The reconstruction and the observations appear to vary more than the simulation.

Wet percentiles for reconstruction and observation evolve oppositely for the short period of overlap (Figure 13a) but dry percentiles agree (Figure 14a). The simulation behaves oppositely for the early part of the data but the trend agrees with the reconstruction for much of the 19th century (Figure 13b). We cannot identify clear commonalities between reconstruction and simulation for the dry percentiles (Figure 14b).

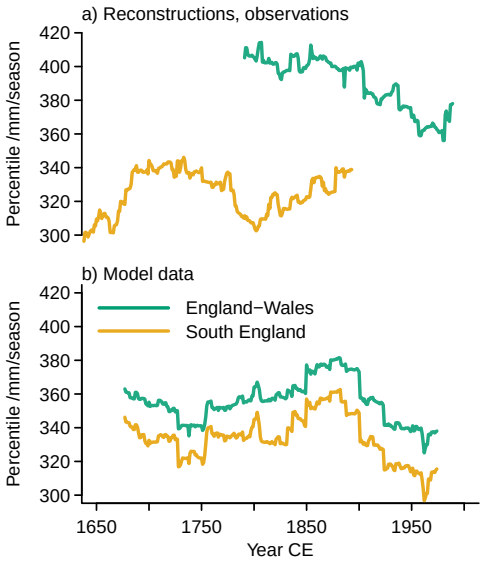

Figure 13: Visualisation of the MJJA precipitation amount identified as severely wet (93.3th percentile) over 51-year windows for a) South England reconstruction and England-Wales observations, and b) regional simulation. England-Wales in green, and South-England in yellow.

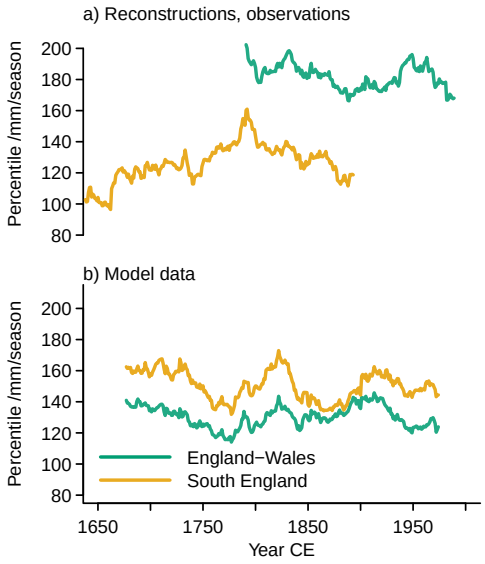

Figure 14: Visualisation of the MJJA precipitation amount identified as severely dry (6.7th percentile) over 51-year windows for a) South England reconstruction and England-Wales observations, and b) regional simulation. England-Wales in green, and South-England in yellow.

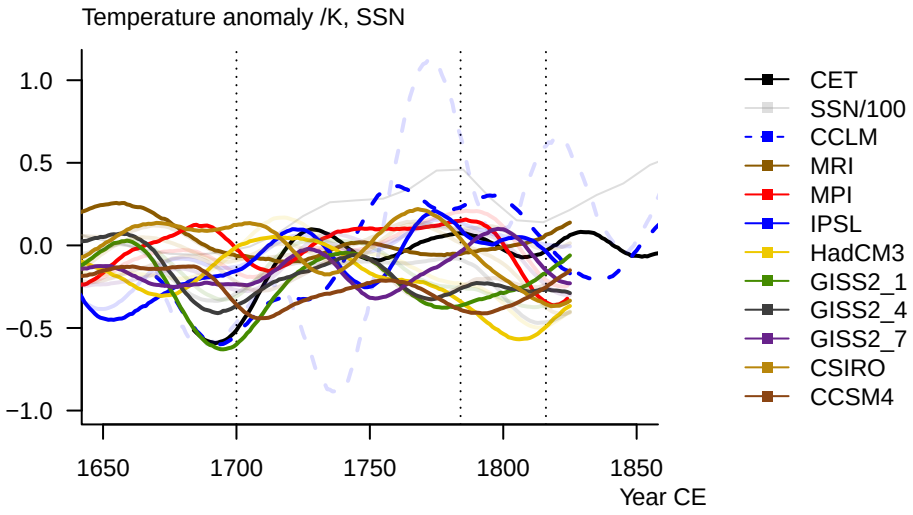

Figure 15: Representations of Central England Temperature for the season March to July smoothed with a 51-point Hamming filter (colored) in various data sets and the Solanki decadal Sunspot Number (SSN, light grey in background, divided by 100, dimensionless): observational Central England Temperature (black solid), CCLM regional simulation (blue dashed), MRI (brown solid), MPI (red solid), IPSL (blue solid), HadCM3 (gold yellow solid), GISS-E2-R 21 (green solid), GISS-E2-R 24 (dark grey solid), GISS-E2-R 27 (dark orchid solid), CSIRO (yellow brown solid), CCSM4 (dark brown solid). Vertical lines give the years 1700, 1784 and 1816 CE.

5 PMIP3-ensemble

We shortly show results for a number of global simulations from the PMIP3-ensemble (Schmidt et al., 2011) for reference. We choose the simulations with CCSM4 (Landrum et al., 2012), CSIRO-Mk3L-1-2 (Phipps et al., 2011), HadCM3 (Schurer et al., 2014), IPSL-CM5A-LR (Dufresne et al., 2013), MPI-ESM (Jungclaus et al., 2014), MRI-CGCM3 (Yukimoto et al., 2012) and the GISS-E2-R ensemble members 21, 24, 27 (Schmidt et al., 2014). For details on the PMIP3 ensemble protocol, see Schmidt et al. (2011).

The global simulations have different grid resolutions. We choose from each simulation the domain including grid points closest to the longitudinal and latitudinal borders 5.5W to 1.5E and 50.5 to 54.5N. This domain choice is somewhat arbitrary but we assume it sufficiently represents the England-Wales precipitation domain to allow meaningful comparison of changes in quantiles, although not in absolute quantile values. The different grids result in different means of seasonally accumulated precipitation in our subsequent analyses. While further model-biases may contribute, we assume the different grids to be the most prominent bias in the accumulated values. We choose the domain 5 to 0W and 50 to 55N as simulated counterparts of the Central England Temperature. Please refer to Wigley et al. (1984) for the definition of the England-Wales precipitation domain for the observational series, and to Parker et al. (1992) for the approximate domain of the observation based Central England Temperature.

Simulation data for the PMIP3-past1000 simulations is available from the nodes of the Earth System Grid Federation, e.g., https://esgf-node.llnl.gov/projects/esgf-llnl/.

5.1 Central England Temperature

Figure 15 presents the representations of the Central England Temperature in the PMIP3-ensemble simulations compared to the observational data and the regional simulation. It shows the 51-year Hamming low-pass filtered temperature records from observations and simulations for the period 1650 to 1850 CE. We show some information about potential external forcings in the Figure as well. Vertical dotted lines represent the years 1700, 1784 (at the end of the volcanic eruption of Laki in 1783/1784), and 1816 CE (the year without a summer after

the eruption of Tambora in 1815 CE). The Figure also adds an estimate of the Sunspot Numbers as light grey line in the background as a measure of solar activity. The data is from Solanki et al. (2004) and divided by 100. It is available at 10-year intervals. Note that we calculate temperature anomalies in this plot over differing periods, i.e. over the full lengths of the respective data sets, because we are only interested in a tentative comparison. These periods are ~850 to 1850 CE for the global simulations, 1645 to 1999 CE for the CCLM data, and 1659 to 2014 CE for the CET data.

The PMIP3 simulation ensemble lacks an obvious common signal and there is not any clear agreement between the simulations and the observations. Internal climate variability from atmospheric, oceanic, and coupled processes is stronger at regional scales than at global scales and, thus, possibly dominates over any potential forced influence.

Note that the regional simulation includes volcanic variations only as reduction in an effective solar constant and uses a rather large solar forcing amplitude. The implementation of the volcanic forcing may lead to climate signals of high latitude eruptions which we would not usually expect, e.g., the late 18th century dip may be due to the Laki eruption on Iceland. D'Arrigo et al. (2011) and Schmidt et al. (2012) report observed heat wave conditions in northern and western Europe in summer 1783 CE. Schmidt et al. (2012) further note that climate simulations did not show such an effect on the European summer climate. The strong warming in the regional simulation may be due to the larger incoming solar radiation forcing in the second half of the 18th century.

5.2 Standardised precipitation in the PMIP3-ensemble

We repeated for the PMIP3-ensemble some of the analyses presented in the main manuscript for the standardized precipitation properties of observations and regional simulation. Figures 16 and 17 visualize the results.

Figure 16 shows for comparison the representation of England-Wales precipitation in a selection of PMIP3 past1000 simulations for the period 1650 to 1850 CE. We again show the data for an extended spring season from March to July. The panels illustrate the diversity of the PMIP3-ensemble including notable opposite anomalies between models and not just unstructured evolutions. These are visible in the smoothed data series in the top panel a) but also in the plots for the percentiles (Figure 16b,c) and the Weibull standard deviation (Figure 16d). For example, the late 18th century is either relatively dry or relatively wet but generally not just in transition (e.g., Figure 16a).

Next, we take MAMJJ precipitation amounts for the 93.3th, 50th, and 6.7th percentiles for the year 1815 CE and consider which percentiles these represent in other time windows. Figure 17 presents these results. We choose 1815 CE as reference year, since it is included in all data sets and it is not yet the last year of the PMIP3 past1000 simulations. The PMIP3-ensemble shows diverse behavior. Most series display some kind of trend of previously increasing or decreasing probability relative to the reference percentile values in the year 1815 CE.

5.3 Correlation between temperature and precipitation in the PMIP3-ensemble

Figure 18 presents interannual correlations over 51-year windows between the representations of the extended spring Central England Temperature and the extended spring England-Wales precipitation in the simulations of the PMIP3 ensemble over the period 1650 to 1850 CE. There is not any common relationship for specific periods or generally between both parameters. Noteworthy are the strong positive relations between temperature and precipitation in two of the GISS-simulations which are in contrast to the observed negative relationship.

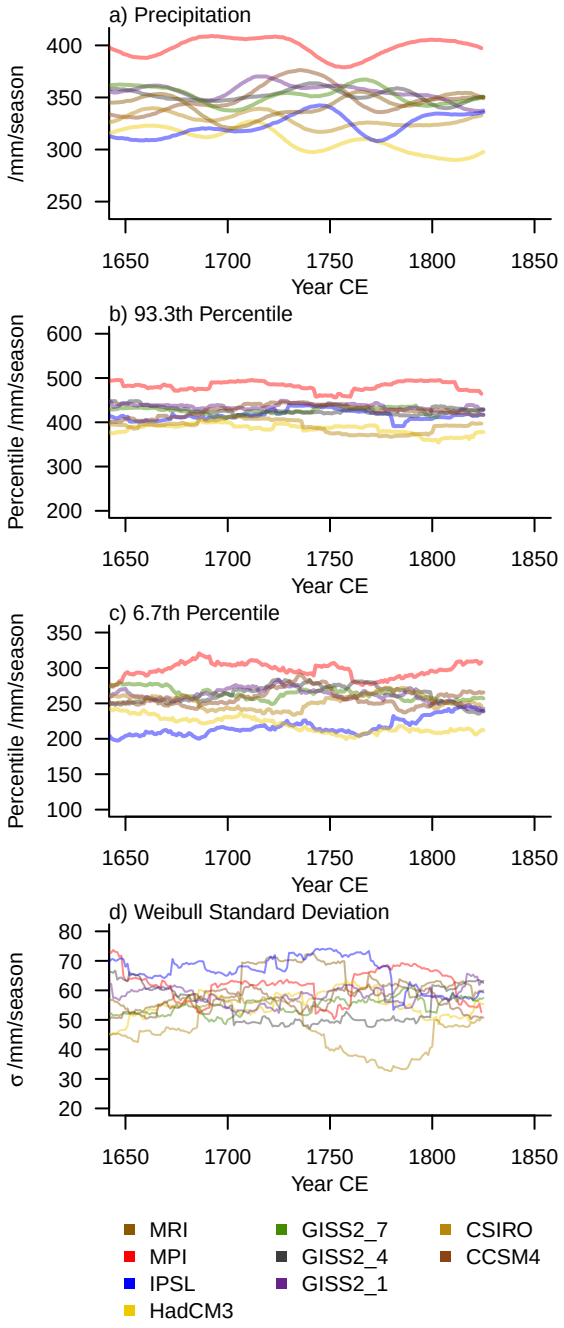

Figure 16: England-Wales extended spring (MAMJJ) precipitation in the PMIP3-ensemble. a) 51-point Hamming-filtered precipitation series. b) 93.3th percentiles calculated over 51-year windows for the data in a). c) 6.7th percentiles calculated over 51-year windows for the data in a). d) Square root of the Weibull distribution variance over 51-year windows for the data in a).

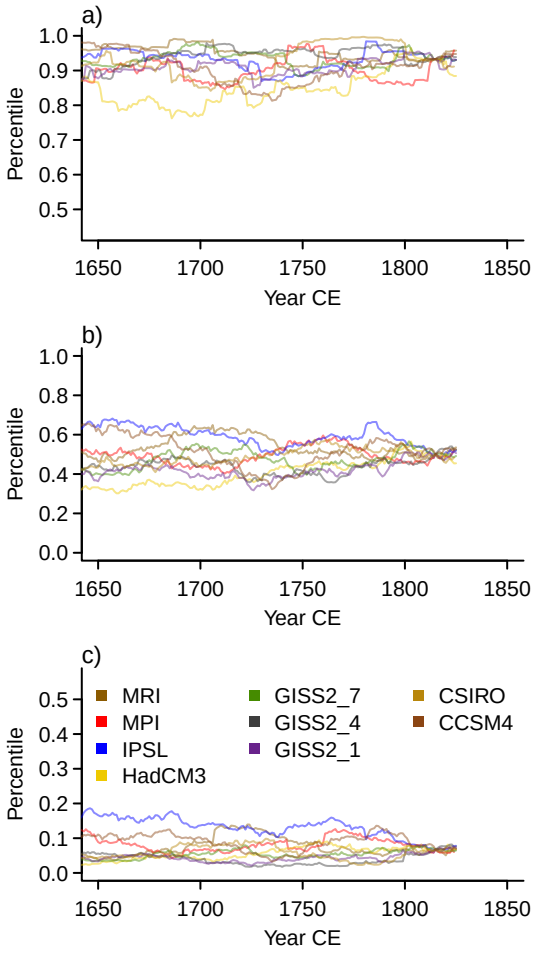

Figure 17: Visualisation of the percentile represented by a reference precipitation amount over time for the members of the PMIP3-ensemble relative to a) the 93.3th percentile for the reference year 1815 CE, b) the 50th percentile for the year 1815 CE, c) the 6.7th percentile for the year 1815 CE. Data is for the extended spring season from March to July.

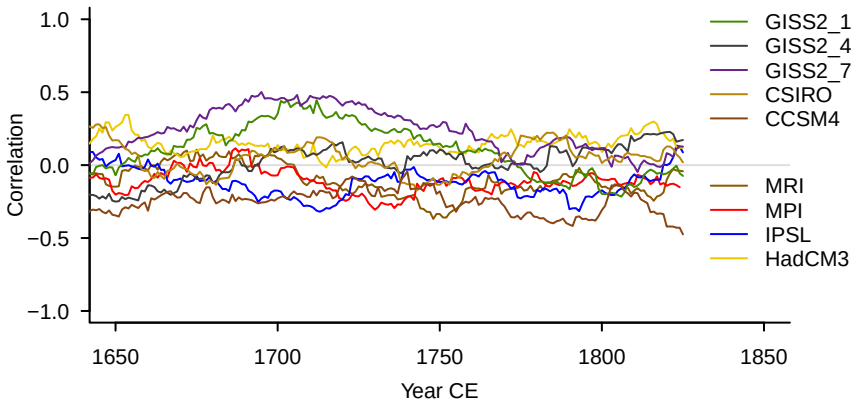

Figure 18: Interannual correlations between Central England temperature and precipitation data over 51-year windows for the PMIP3-ensemble over the period 1650 to 1850 CE. All data are for the extended spring season from March to July.

6 Acknowledgements

We acknowledge the help of Katja Rinne-Garmston, who provided the reconstruction of Rinne et al. (2013). We further acknowledge the service of the ESGF for providing the PMIP3-simulations.

References

Alexander, L. V. and Jones, P. D.: Updated precipitation series for the U.K. and discussion of recent extremes, Atmosph. Sci. Lett., 1, 142–150, https://doi.org/10.1006/asle.2000.0016, 2000.

D'Arrigo, R., Seager, R., Smerdon, J. E., LeGrande, A. N., and Cook, E. R.: The anomalous winter of 1783–1784: Was the Laki eruption or an analog of the 2009–2010 winter to blame?, Geophys. Res. Lett., 38, L05 706+, https://doi.org/10.1029/2011gl046696, 2011.

Dufresne, J. L., Foujols, M. A., Denvil, S., Caubel, A., Marti, O., Aumont, O., Balkanski, Y., Bekki, S., Bellenger, H., Benshila, R., Bony, S., Bopp, L., Braconnot, P., Brockmann, P., Cadule, P., Cheruy, F., Codron, F., Cozic, A., Cugnet, D., de Noblet, N., Duvel, J. P., Ethé, C., Fairhead, L., Fichefet, T., Flavoni, S., Friedlingstein, P., Grandpeix, J. Y., Guez, L., Guilyardi, E., Hauglustaine, D., Hourdin, F., Idelkadi, A., Ghattas, J., Joussaume, S., Kageyama, M., Krinner, G., Labetoulle, S., Lahellec, A., Lefebvre, M. P., Lefevre, F., Levy, C., Li, Z. X., Lloyd, J., Lott, F., Madec, G., Mancip, M., Marchand, M., Masson, S., Meurdesoif, Y., Mignot, J., Musat, I., Parouty, S., Polcher, J., Rio, C., Schulz, M., Swingedouw, D., Szopa, S., Talandier, C., Terray, P., Viovy, N., and Vuichard, N.: Climate change projections using the IPSL-CM5 Earth System Model: from CMIP3 to CMIP5, Climate Dynamics, 40, 2123–2165, https://doi.org/10.1007/s00382-012-1636-1, 2013.

Jungclaus, J. H., Lohmann, K., and Zanchettin, D.: Enhanced 20th-century heat transfer to the Arctic simulated in the context of climate variations over the last millennium, Climate of the Past, 10, 2201–2213, https://doi.org/10.5194/cp-10-2201-2014, 2014.

Landrum, L., Otto-Bliesner, B. L., Wahl, E. R., Conley, A., Lawrence, P. J., Rosenbloom, N., and Teng, H.: Last Millennium Climate and Its Variability in CCSM4, J. Climate, 26, 1085–1111, https://doi.org/10.1175/jcli-d-11-00326.1, 2012.

Parker, D. E., Legg, T. P., and Folland, C. K.: A new daily central England temperature series, 1772–1991, Int. J. Climatol., 12, 317–342, https://doi.org/10.1002/joc.3370120402, 1992.

Phipps, S. J., Rotstayn, L. D., Gordon, H. B., Roberts, J. L., Hirst, A. C., and Budd, W. F.: The CSIRO Mk3L climate system model version 1.0 - Part 1: Description and evaluation, Geoscientific Model Development, 4, 483–509, https://doi.org/10.5194/gmd-4-483-2011, 2011.

Rinne, K., Loader, N., Switsur, V., and Waterhouse, J.: 400-year May–August precipitation reconstruction for Southern England using oxygen isotopes in tree rings, Quaternary Science Reviews, 60, 13–25, https://doi.org/10.1016/j.quascirev.2012.10.048, 2013.

Schmidt, A., Thordarson, T., Oman, L. D., Robock, A., and Self, S.: Climatic impact of the long-lasting 1783 Laki eruption: Inapplicability of mass-independent sulfur isotopic composition measurements, J. Geophys. Res., 117, D23 116+, https://doi.org/10.1029/2012jd018414, 2012.

Schmidt, G. A., Jungclaus, J. H., Ammann, C. M., Bard, E., Braconnot, P., Crowley, T. J., Delaygue, G., Joos, F., Krivova, N. A., Muscheler, R., Otto-Bliesner, B. L., Pongratz, J., Shindell, D. T., Solanki, S. K., Steinhilber, F., and Vieira, L. E. A.: Climate forcing reconstructions for use in PMIP simulations of the last millennium (v1.0), Geoscientific Model Development, 4, 33–45, https://doi.org/10.5194/gmd-4-33-2011, 2011.

Schmidt, G. A., Kelley, M., Nazarenko, L., Ruedy, R., Russell, G. L., Aleinov, I., Bauer, M., Bauer, S. E., Bhat, M. K., Bleck, R., Canuto, V., Chen, Y.-H., Cheng, Y., Clune, T. L., Del Genio, A., de Fainchtein, R., Faluvegi, G., Hansen, J. E., Healy, R. J., Kiang, N. Y., Koch, D., Lacis, A. A., LeGrande, A. N., Lerner, J., Lo, K. K., Matthews, E. E., Menon, S., Miller, R. L., Oinas, V., Oloso, A. O., Perlwitz, J. P., Puma, M. J., Putman, W. M., Rind, D., Romanou, A., Sato, M., Shindell, D. T., Sun, S., Syed, R. A., Tausnev, N., Tsigaridis, K., Unger, N., Voulgarakis, A., Yao, M.-S., and Zhang, J.: Configuration and assessment of the GISS ModelE2 contributions to the CMIP5 archive, Journal of Advances in Modeling Earth Systems, 6, 141–184, https://doi.org/10.1002/2013ms000265, 2014.

Schurer, A. P., Tett, S. F. B., and Hegerl, G. C.: Small influence of solar variability on climate over the past millennium, Nature Geosci, 7, 104–108, https://doi.org/10.1038/ngeo2040, 2014.

Solanki, S. K., Usoskin, I. G., Kromer, B., Schussler, M., and Beer, J.: Unusual activity of the Sun during recent decades compared to the previous 11,000 years, Nature, 431, 1084–1087, https://doi.org/10.1038/nature02995, 2004.

Wigley, T. M. L., Lough, J. M., and Jones, P. D.: Spatial patterns of precipitation in England and Wales and a revised, homogeneous England and Wales precipitation series, J. Climatol., 4, 1–25, https://doi.org/10.1002/joc.3370040102, 1984.

Young, G. H. F., Loader, N. J., McCarroll, D., Bale, R. J., Demmler, J. C., Miles, D., Nayling, N. T., Rinne, K. T., Robertson, I., Watts, C., and Whitney, M.: Oxygen stable isotope ratios from British oak tree-rings provide a strong and consistent record of past changes in summer rainfall, Climate Dynamics, 45, 3609–3622, https://doi.org/10.1007/s00382-015-2559-4, 2015.

Yukimoto, S., Adachi, Y., Hosaka, M., Sakami, T., Yoshimura, H., Hirabara, M., Tanaka, T. Y., Shindo, E., Tsujino, H., Deushi, M., Mizuta, R., Yabu, S., Obata, A., Nakano, H., Koshiro, T., Ose, T., and Kitoh, A.: A New Global Climate Model of the Meteorological Research Institute: MRI-CGCM3 – Model Description and Basic Performance—, Journal of the Meteorological Society of Japan. Ser. II, 90A, 23–64, https://doi.org/10.2151/jmsj.2012-A02, 2012.